


# High adsorption and separation performance of $CO_2$ over $N_2$ in azo-based (N=N) pillar[6]arenesupramolecular organic frameworks

Yong-Chao Jiang(姜永超), Gui-Xia Li(李桂霞), Gui-Feng Yu(于桂凤), Juan Wang(王娟), Shu-Lai Huang(黄树来), and Guo-Liang Xu(徐国亮)

**Citation:**Chin. Phys. B, 2021, 30 (**11**): 118105. DOI: 10.1088/1674-1056/ac05b5
Journal homepage: http://cpb.iphy.ac.cn; http://iopscience.iop.org/cpb

**What follows is a list of articles you may be interested in**

---

## Adsorption of $CO_2$ on MgAl layered double hydroxides: Effect of intercalated anion and alkaline etching time

Yan-Yan Feng(冯艳艳), Xiao-Di Niu(牛潇迪), Yong-Hui Xu (徐永辉), and Wen Yang(杨文)
Chin. Phys. B, 2021, 30 (**4**): 048101. DOI: 10.1088/1674-1056/abd750

## Influence of an inserted bar on the flow regimes in the hopper

Yi Peng(彭毅), Sheng Zhang(张晟), Mengke Wang(王梦柯), Guanghui Yang(杨光辉), Jiangfeng Wan(万江锋), Liangwen Chen(陈良文), and Lei Yang(杨磊)
Chin. Phys. B, 2021, 30 (**2**): 028101. DOI: 10.1088/1674-1056/abcf40

## Prediction of structured void-containing 1T-$PtTe_2$ monolayer with potential catalytic activity for hydrogen evolution reaction

Bao Lei(雷宝), Yu-Yang Zhang(张余洋), Shi-Xuan Du(杜世萱)
Chin. Phys. B, 2020, 29 (**5**): 058104. DOI: 10.1088/1674-1056/ab8203

## Overview of finite elements simulation of temperature profile to estimate properties of materials 3D-printed by laser powder-bed fusion

Habimana Jean Willy, Xinwei Li(李辛未), Yong Hao Tan, Zhe Chen(陈哲), Mehmet Cagirici, Ramadan Borayek, Tun Seng Herng, Chun Yee Aaron Ong, Chaojiang Li(李朝将), Jun Ding(丁军)
Chin. Phys. B, 2020, 29 (**4**): 048101. DOI: 10.1088/1674-1056/ab6d4e

## Silicon nanoparticles： Preparation, properties, and applications

Chang Huan, Sun Shu-Qing
Chin. Phys. B, 2014, 23 (**8**): 088102. DOI: 10.1088/1674-1056/23/8/088102

---

# High adsorption and separation performance of $CO_2$ over $N_2$ in azo-based (N=N) pillar[6]arene supramolecular organic frameworks*

Yong-Chao Jiang(姜永超)[1], Gui-Xia Li(李桂霞)[1], Gui-Feng Yu(于桂凤)[1], Juan Wang(王娟)[1], Shu-Lai Huang(黄树来)[1], and Guo-Liang Xu(徐国亮)[2,†]

[1] *College of Science and Information, Qingdao Agricultural University, Qingdao* 266109, *China*
[2] *School of Physics, Henan Normal University, Xinxiang* 453007, *China*

(Received 27 February 2021; revised manuscript received 13 May 2021; accepted manuscript online 27 May 2021)

Azo-based pillar[6]arene supramolecular organic frameworks are reported for $CO_2$ and $N_2$ adsorption and separation by density functional theory and grand canonical Monte–Carlo simulation. Azo-based pillar[6]arene provides suitable environment for $CO_2$ adsorption and selectivity. The adsorption and selectivity results show that introducing azo groups can effectively improve $CO_2$ adsorption and selectivity over $N_2$, and both $CO_2$ adsorption and $CO_2$ selectivity over $N_2$ follow the sequence pillar[6]arene_N4 > pillar[6]arene_N2 > pillar[6]arene. Pillar[6]arene_N4 exhibits $CO_2$ adsorption capacity of $\sim 1.36$ mmol/g, and superior selectivity of $CO_2$ over $N_2$ of $\sim 116.75$ with equal molar fraction at 1 bar (1 bar $= 10^5$ Pa) and 298 K. Interaction analysis confirms that both the Coulomb and van der Waals interactions between $CO_2$ with pillar[6]arene frameworks are greater than that of $N_2$. The stronger affinity of $CO_2$ with pillar[6]arene_N4 than other structures and the larger isosteric heat differences between $CO_2$ and $N_2$ rendered pillar[6]arene_N4 to present the high $CO_2$ adsorption capacity and high $CO_2$ selectivity over $N_2$. Our results highlight the potential of azo-functionalization as an excellent means to improve pillar[6]arene for $CO_2$ capture and separation.

**Keywords:** supramolecular organic framework, functionalization, modelling and simulation, carbon capture and storage

**PACS:** 81.05.Rm, 68.43.–h, 31.15.E, 05.10.Ln **DOI:** 10.1088/1674-1056/ac05b5

## 1. Introduction

The rapid climate change caused by global warming has been a serious issue due to the extensive $CO_2$ emission into the atmosphere by anthropogenic activities such as industrial production, power plants emission, and vehicle emissions.[1] The development of efficient strategies is more challenging, and becomes an urgent task to mitigate the global warming and to continue to use fossil fuels. Under such a background, carbon capture and storage (CCS) technologies play a critical process to tackle this urgent globally environmental problem by capture and separation of $CO_2$.[2] In order to obtain high efficiency of CCS, it is highly desirable that the suitable materials serving as effective adsorbent is utilized for $CO_2$ capture and separation.[3] Supramolecular organic frameworks with intrinsic porosity, based on the assembly of calixarenes,[4] bisurea,[5] cucurbiturils,[6] and more recently pillarenes,[7,8] have emerged as a excellent solid adsorbent materials for $CO_2$ adsorption and separation. Among them, pillar[n]arene has been exploited as an excellent candidate for $CO_2$ capture and separation because of high thermal stability, favourable pore characteristics and good gas sorption properties.

As a desired gas adsorption material, pillar[*n*]arene has been experiencing comprehensive and substantial studies on its structures, properties, and syntheses. Ogoshi *et al.* adopted per-hydroxylated pillar[6]arene to capture gas and vapour, and found 1D channels of the per-hydroxylated pillar[6]arene can adsorb various gases and organic vapours due to their pillar-shaped structures with suitable pore volume of 0.098 $cm^3/g$.[9] Tan *et al.* investigated pillar[6]arene for selective sorption of hydrocarbons, and found that P5-SOF has good selectively of $C_2H_2$ over $H_2$ ($\sim 2969/1$), $C_2H_6$ ($\sim 295/1$), $N_2$ ($\sim 60/1$), $CH_4$ ($\sim 41/1$), and $C_2H_4$ ($\sim 20/1$) and exhibits high selectivity for other gas mixtures under the equimolar gas mixture condition at 1.0 bar.[10] Tan *et al.* employed pillar[5]arene and pillar[6]arene to realize high selective $CO_2$ adsorption capacity for $CO_2/H_2$ mixtures, reaching up to $3733/1$ for $30/70$ mixture of $CO_2/H_2$ at 298 K via strong O–H$\cdots$O, C–H$\cdots$O, C–H$\cdots\pi$, $\pi\cdots\pi$ interactions.[11] Therefore, pillar[n]arene might be deemed to possess outstanding gas capture performance with strong gas–framework interaction. So far as we know, the effects of functionalization, the improvement mechanism on the $CO_2$ adsorption and selectivity over $CO_2$ of $N_2$ mixture gas in functionalized pillar[6]arenes materials have not been distinctly explained.

In this work, we adopt azo group (N=N) to decorate pillar[6]arene for investigating the adsorption and separation performance of $CO_2/N_2$ mixture by density functional theory

*Project supported by Shandong Province Higher Education Science and Technology Program, China (Grant No. J17KA016), State Key Laboratory of Bio-Fibers and Eco-Textiles (Grant No. K2019-12), and the Cultivation Fund of Henan Normal University, China (Grant No. 2020PL15).

†Corresponding author. E-mail: xugliang@htu.edu.cn

© 2021 Chinese Physical Society and IOP Publishing Ltd 

(DFT) and grand canonical Monte–Carlo (GCMC). Firstly, we optimize the geometry structure of functionalized pillar[6]arenes and calculate their atomic partial charge as the basic input parameters in GCMC simulation by DFT; secondly, the functionalized pillar[6]arenes pore characteristics of the azo-based pillar[6]arenes are showed; thirdly, adsorption capacity and separation of $CO_2/N_2$ mixture is calculated; finally, the isosteric heats, interaction energy, and adsorption energy are analyzed to determine the effects of azo-functionalization on the adsorption strength and characteristics. Our results highlight the potential use of the azo-based pillar[6]arenes in CCS for high adsorption capacity and high selectivity of $CO_2$ over $N_2$.

## 2. Model and methodology

Pillar[6]arene was adopted as the initial unit to form the adsorbing material for separating $CO_2$ from $CO_2/N_2$ mixture. Firstly, we assumed that the incorporation of azo group into the macrocyclic backbone of pillar[6]arene: pillar[6]arene_N2, which have two decorated macrocyclic backbones; pillar[6]arene_N4, which have four decorated macrocyclic backbones, as shown in Fig. 1. After building these three structures, optimizing structure and analyzing atomic charge were carried out by means of DFT. The B3LYP/6-31+g(d,p) basis was set in Gaussian 09 package with the highly computational efficiency and sufficient accuracy.[12] The self-consistent field (SCF) was computed with a convergence threshold of $10^{-6}$ a.u. on total energy. Next, their functionalized pillar[6]arene frameworks were composed by four well-ordered optimized units. Atomic partial charges (ChelpG) of functionalized pillar[6]arenes were used as important information parameters in GCMC simulations to describe the electrostatic interaction by Coulomb law.

$CO_2$ and $N_2$ molecules were regarded as rigid linear molecules, and the three-site molecule was used for $CO_2$ and $N_2$ molecules. The LJ potential parameters for both $CO_2$ and $N_2$ molecules were obtained from the TraPPE model, which were reported by Potoff and Siepmann.[13] Dreiding force field[14] was applied to acquire atomic Lennard–Jones 12–6 potential ($U_{LJ}$) parameters. This force field has been successfully appropriated for a wealth of adsorbed materials, such as $CN_n$ sheets,[15] metal organic frameworks (MOFs),[16] and boron nitride nanotube.[17] GCMC simulations were employed to calculate the uptake of single-component $CO_2$ and $N_2$, and the selectivity of $CO_2$ over $N_2$ in their binary mixture with different ratio in functionalized pillar[6]arene. Lennard–Jones 12–6 potential was used to describe the van der Waals interaction, which is calculated as follows:

$$U_{LJ} = 4\varepsilon_{ij}\left[\left(\frac{\sigma_{ij}}{r_{ij}}\right)^6 - \left(\frac{\sigma_{ij}}{r_{ij}}\right)^{12}\right], \tag{1}$$

where $r_{ij}$, $\varepsilon_{ij}$, and $\sigma_{ij}$ are the collision diameter, potential well depth, and distance between sites $i$ and $j$, respectively. The cross interactions between unlike atoms are calculated by the Lorentz–Berthelot combining rules given as follows:

$$\sigma_{ij} = \frac{1}{2}(\sigma_{ii} + \sigma_{jj}), \tag{2}$$

$$\varepsilon_{ij} = \sqrt{\varepsilon_{ii} \cdot \varepsilon_{jj}}. \tag{3}$$

And the Coulomb law was used to calculate the electrostatic interaction, which is as follows:

$$E_{\text{Coulomb}} = \frac{e^2}{4\pi\varepsilon_0}\sum_{i\neq j}\frac{q_i q_j}{r_{ij}}, \tag{4}$$

where the charge on particles $i$ and $j$ are $q_i$ and $q_j$, respectively, in units of $e$. The dielectric constant at vacuum condition is represented by $\varepsilon_0$ with the value of $8.85 \times 10^{-12}$ F/m. For the GCMC simulations, 100000 cycles were used in which the first 50000 cycles were used for initialization, and the last 50000 cycles were performed for taking ensemble averages. All these GCMC simulations were implemented in the RASPA simulation code.[18]

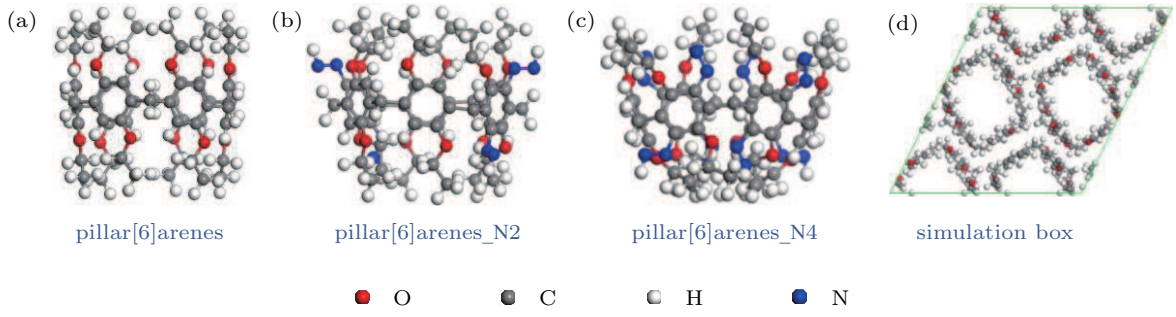



**Fig. 1.** Initial configurations of the azo-based pillar[6]arenes.

## 3. Results and discussion

### 3.1. Pore topology and morphology

Pore structure of frameworks is a decisive factor for gas adsorption and separation. We use Poreblazer v3.0[19] to evaluate the available pore volume ($V_P$), pore limiting diameter ($D_L$), maximum pore diameter ($D_M$), and accessible surface area. The porosity ($\Phi$) is estimated by $V_P/V_{Total}$, where $V_{Total}$ is the total volume of the frameworks. Table 1 lists the pore structure of the three functionalized pillar[6]arene

evaluated, which were reported by Sarkisov[20] and Duren[21] methods. After decorating, the density increase to 1.184 g·cm$^{-3}$ from the original 0.979 g·cm$^{-3}$, and more $N$ atoms are introduced into frameworks leading to the greater density. The $V_p$ of the azo-based pillar[6]arene fluctuate from 0.32 cm$^3$/g to 0.43 cm$^3$/g, which are lower than those of the unmodified pillar[6]arene. The accessible surface areas of the azo-based pillar[6]arene decrease from 1073.36 m$^2$·g$^{-1}$ to 880.54 m$^2$·g$^{-1}$ with the increasing of the azo group number, and these values are larger than those of traditional adsorbent zeolite 13X (591 m$^2$·g$^{-1}$),[22] a part of metal−organic materials (200–300 m$^2$·g$^{-1}$),[23] similar to some 2D covalent organic frameworks (688–1197 m$^2$·g$^{-1}$),[24] but lower than those of metal organic frameworks with high porosity ($\sim$ 6000 m$^2$·g$^{-1}$).[25] The porosity of three azo-based pillar[6]arenes is kept about 30%. In contrast with pillar[6]arene, azo-functionalization has little effect on $D_L$ and $D_M$.

**Table 1.** Physical characteristics of the azo-based pillar[6]arenes (gas probe molecule = He with diameter of 2.58 Å).

| Parameter | Pillar[6]arene | Pillar[6]arene_N2 | Pillar[6]arene_N4 |
|---|---|---|---|
| Density (g/cm$^3$) | 0.98 | 1.08 | 1.18 |
| Porosity | 34.2% | 31% | 28.9% |
| Surface area (m$^2$/g) | 1073.36 | 937.25 | 880.54 |
| $V_p$ (cm$^3$/g) | 0.43 | 0.35 | 0.32 |
| $D_L$ (Å) | 4.24 | 3.96 | 4.24 |
| $D_M$ (Å) | 6.09 | 3.96 | 6.09 |

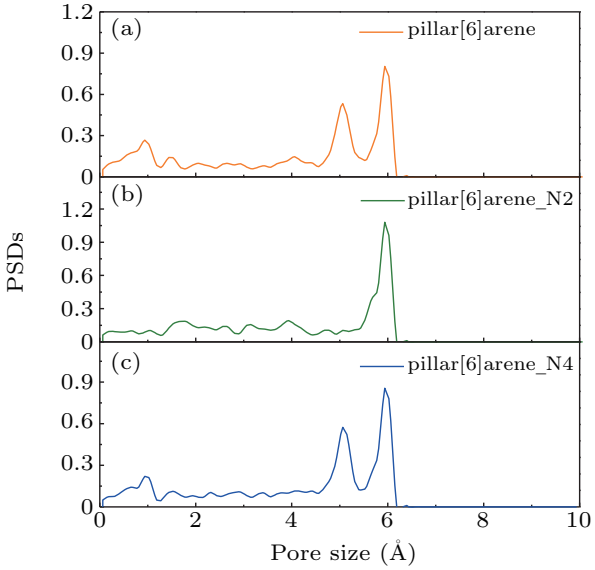



**Fig. 2.** The pore size distributions of the azo-based pillar[6]arenes.

To gain a deeper insight into the pore morphological structures, the pore size distributions (PSDs) are showed in Fig. 2. All PSDs present similar continuous distribution, and all pore sizes are smaller than 7 Å, which are the typical ultramicropore structures (< 7.00 Å) in accordance with the IUPAC classification.[26] The main pore distributions concentrate on 5–6 Å. The PSDs findings demonstrate the unmodified pillar[6]arene exist some pore, which is smaller than 2 Å. Based on the previous work, pores with sizes of 5–7 Å or even below (also referred to as ultramicropores) should be presented because they have a larger adsorption potential for $CO_2$ as compared to larger supermicropores (7–20 Å) or mesopores (> 2 nm)[1] at the low-pressure. Therefore, three azo-based pillar[6]arenes provide favorable environment for $CO_2$ adsorption and separation.

### 3.2. Single-component adsorption of $CO_2/N_2$

Single-component adsorption capacity is the primary standard to evaluate the adsorbent performance. The absolute adsorption isotherms of the single-component $CO_2$ adsorption in three azo-based pillar[6]arenes at 298 K are presented in Fig. 3(a). The absolute $CO_2$ adsorption capacities in the azo-based pillar[6]arenes are significantly higher than that of the unmodified pillar[6]arenes. At 1 bar, the adsorption capacity of three azo-based pillar[6]arenes is 0.66 mmol/g for pillar[6]arene, 0.75 mmol/g for pillar[6]arene_N2, and 1.36 mmol/g for pillar[6]arene_N4, respectively. The results show that azo-functionalization can improve the adsorption capacity of pillar[6]arene. In particular, pillar[6]arene_N4 presents larger adsorption capacity, which is larger than those of typical supramolecular organic framework T-SOF-1 ($\sim$ 1.07 mmol/g),[27] TPP (0.94 mmol/g),[4] DMP5-SOF (0.05 mmol/g),[28] SMOF-SIFSIX-1a (1.05 mmol/g)[29] and B2 ($\sim$ 0.67 mmol/g),[4] and MgAl(Cl) ($\sim$ 0.136),[28] but smaller than nanoporous carbons (2.14–9.62 mmol/g),[30] and similar to azo based COF-TpAzo (1.59 mmol/g) at the same conditions. The increased $CO_2$ uptake performances are attributed to the introduction of azo groups, which add strong adsorption sites, change pore topology, and strengthen interactions with $CO_2$ and $N_2$ molecules. Introducing azo groups leads to the increasing of the number of N atoms in the frameworks. That is, an azo group (N=N) with large electronegativity increases interactions with $CO_2$ molecules of strong electric quadrupole moment.

Figure 3(b) shows the absolute adsorption isotherms of $N_2$ in the azo-based pillar[6]arenes at 298 K. Pillar[6]arene_N2 with two decorated macrocyclic backbones has a slight impact on adsorption capacity of $N_2$. The adsorption capacity of $N_2$ has improvement in pillar[6]arene_N4 frameworks. At 1 bar, the pillar[6]arene_N4 presents the highest adsorption capacity (0.053 mmol/g), which is far less than most of traditional adsorbent materials, such as, 13X zeolites,[31] similar to azo based COF-TpAzo ($\sim$ 0.051 mmol/g), and larger than a family of azo-bridged covalent organic polymers (azo-COPs) (0.03–0.05 mmol/g) at the same conditions. For the temperature effect, the gas adsorption capacity decreases along with the increase of temperature as a result of the exothermic nature of the adsorption process. For instance, at the pressures above 1 bar, the total $CO_2$ uptakes in azo-based

pillar[6]arenes are within the range of 0.66–1.36 and 1.12–1.66 mmol/g at 298 and 273 K, respectively (see Figs. 3(a) and 3(c)).

Overall, the adsorption of $CO_2/N_2$ in the azo-based pillar[6]arenes exhibits type-I Langmuir adsorption behavior, which is a typical characteristic of microporous adsorption.[32] The azo groups significantly enhance the adsorption capacities of $CO_2$. In particular, the results show that the pillar[6]arene_N4 processes the better adsorption capacity of $CO_2$ and weaker adsorption capacity of $N_2$, which compare with congeneric supramolecular frameworks.

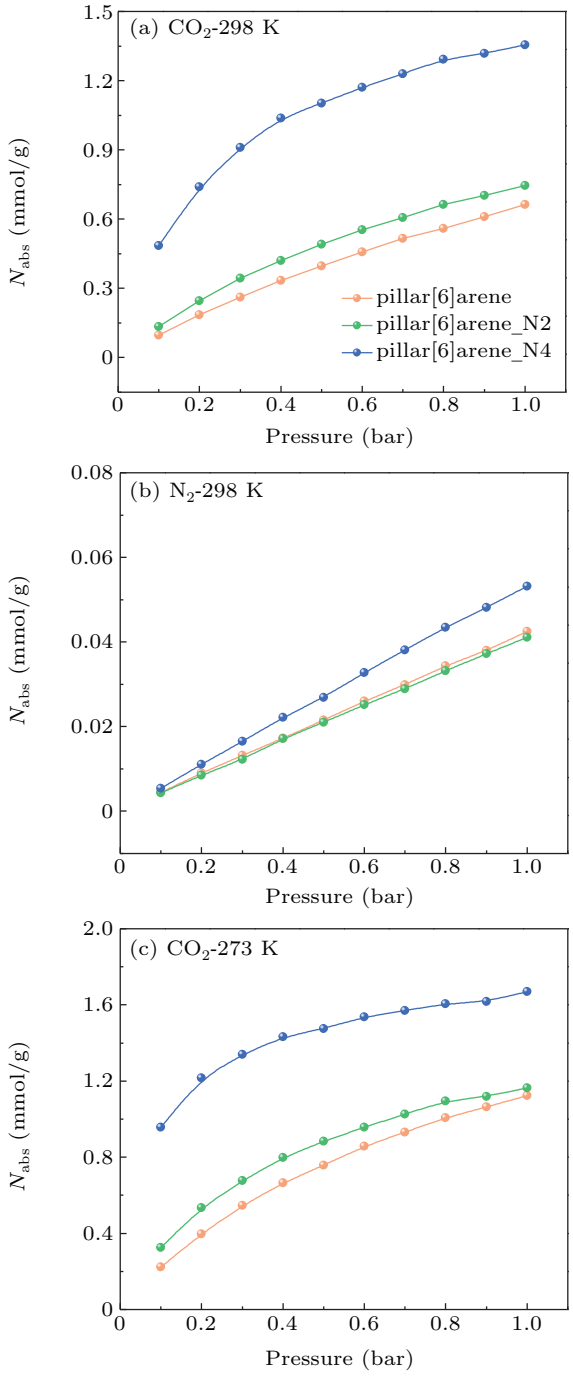



**Fig. 3.** (a) Absolute adsorption isotherms of $CO_2$ at 298 K. (b) $N_2$ in the azo-based pillar[6]arenes at 298 K. (c) Absolute adsorption isotherms of $CO_2$ at 273 K.

### 3.3. Selectivity of $CO_2$ over $N_2$ with equal molar fraction

The selectivity of $CO_2$ over $N_2$ is the important criterion to screen superior adsorbent materials to separate $CO_2$ from the $CO_2/N_2$ mixtures. The selectivity of $CO_2$ over $N_2$ is defined as

$$S_{CO_2/N_2} = (x_{CO_2}/x_{N_2})/(y_{CO_2}/y_{N_2}), \tag{5}$$

where $S$ is the selectivity of $CO_2$ over $N_2$, $x_{CO_2}$ and $x_{N_2}$ are the molar fractions of $CO_2$ and $N_2$ in their adsorbed phase, and $y_{CO_2}$ and $y_{N_2}$ are the corresponding molar fractions of $CO_2$ and $N_2$ in their bulk gas phases. The selectivity of $CO_2$ over $N_2$ with equal molar fraction in the azo-based pillar[6]arenes at 298 K are showed in Fig. 4(a).

The selectivity of $CO_2$ over $N_2$ declines initially, and then flattens out to a constant value with the increase in pressure. At 298 K and 1 bar, the selectivity of $CO_2$ over $N_2$ decreases in the sequence of pillar[6]arene_N4 ($\sim$ 116) > pillar[6]arene_N2 ($\sim$ 32) > pillar[6]arene ($\sim$ 27). Pillar[6]arene_N4 exhibits the best selectivity, which is better than that of azo-UiO-66 ($\sim$ 100),[33] azo-COP-*X* (*X* = 1–3) ($\sim$ 65–130),[34] and traditional Zr-BFDC ($\sim$ 60),[35] and ZIF-8 ($\sim$ 4).[36] The results show that pillar[6]arene_N4 have a distinct advantage over other adsorption materials. This is ascribed that the introducing azo groups (N=N) can provide the stronger attractive interactions between $CO_2$ and the framework than that of $N_2$. $CO_2$ has stronger quadrupole moment ($4.30 \times 10^{26}$ esu·cm$^2$) and polarizability ($2.91 \times 10^{25}$ cm$^3$), while $N_2$ have weaker quadrupole moment ($1.52 \times 10^{26}$ esu·cm$^2$) and polarizability ($1.74 \times 10^{25}$ cm$^3$).[37] So, $CO_2$ has the stronger electrostatic interaction with frameworks than that of $N_2$. In addition, the pore sizes focus on ultramicropores (< 7 Å), which is the optimum size for separate $CO_2/N_2$ mixtures. $CO_2$ has preferential adsorption behavior to fill the optimal adsorption sites, whereafter, $N_2$ has no void space to adsorb into frameworks due to smaller pore sizes.

The separation of $CO_2$ from $N_2$ is an essential step in power plant ("post-combustion") flue-gas purification. Flue gases typically contain 3%–15% $CO_2$ and more than 70% $N_2$.[38] In order to be closer to the practical production and life, $CO_2/N_2$ mixture gases with 15:85 ratio are taken into account. Figure 4(b) shows the selectivities of $CO_2$ over $N_2$ in non-equimolar $CO_2/N_2$ mixtures with ratios of 15:85. Overall, the selectivities of $CO_2$ over $N_2$ in non-equimolar $CO_2/N_2$ mixtures show a similar trend to that in equimolar $CO_2/N_2$ mixtures. And the sequence of selectivity in the azo-based pillar[6]arenes is pillar[6]arene_N4 ($\sim$ 132) > pillar[6]arene_N2 ($\sim$ 36) > pillar[6]arene ($\sim$ 28), which shows its sequence is not affected by molar fraction of $CO_2/N_2$ mixture. Compared with azo decorated structures, pillar[6]arene_N4 has superior selectivity of $CO_2$ than that of nanoporous azo-linked polymers ($\sim$ 25–38)[39] and some azo-COPs ($\sim$ 95–130)[40] at the

same conditions. Moreover, the selectivity of $CO_2$ over $N_2$ in pillar[6]arene_N4 is higher than that of traditional materials, such as, JLU-Liu46-47 ($\sim$ 50),[41] edge-functionalized nanoporous carbons ($\sim$ 3–130) at 298 K,[30] and ordered carbon nanotube arrays (3–65) at 303 K.[42] As a whole, the azo-based pillar[6]arenes can provide a high single-component adsorption capacity and selectivity of $CO_2/N_2$, and thus exhibit a promising potential for CCS technology.

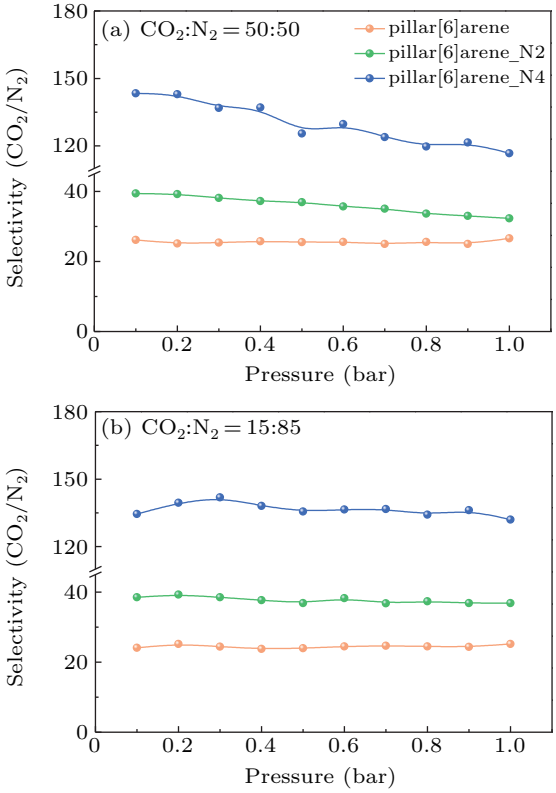



**Fig. 4.** Selectivity of $CO_2$ over $N_2$ in the azo-based pillar[6]arenes at 298 K with the different mixture ratios of $CO_2/N_2$, (a) 50:50, (b) 15:85.

### 3.4. Mechanism of $CO_2/N_2$ adsorption and separation

To deepen our understanding of intrinsic mechanisms of $CO_2/N_2$ adsorption and separation in the azo-based pillar[6]arenes, isosteric heats ($Q_{st}$), interaction analyses, the most stable adsorption configuration and the corresponding maximum adsorption energy are presented.

The $Q_{st}$ is the critical parameter to illustrate the interaction strength between $CO_2/N_2$ and frameworks. $Q_{st}$ is calculated by the Clausius–Clapeyron formula

$$(\ln P)_N = -(Q_{st}/R)(1/T) + C, \tag{6}$$

where $T$ represents temperature, $P$ represents pressure, $N$ represents the number of adsorbate molecules, $R$ represents the ideal gas constant, and $C$ represents a constant. As shown in Fig. 5, the $Q_{st}$ of $CO_2$ is $\sim$ 25 kJ·mol$^{-1}$ in the pillar[6]arene at the 0–1.0 bar, whereas $Q_{st}$ of $CO_2$ increases to $\sim$ 27 kJ·mol$^{-1}$ for pillar[6]arene_N2 and $\sim$ 33 kJ·mol$^{-1}$ for pillar[6]arene_N4 due to N=N group introducing. The results show the weak physisorption are formed between $CO_2$ and the azo-based pillar[6]arenes, according to its adsorption strength definition of 25–50 kJ·mol$^{-1}$.[43] Comparing with $CO_2$, $Q_{st}$ of $N_2$ is apparently smaller, and this result is attributed to the stronger interactions between $CO_2$ with strong electric quadrupole moment and frameworks. The sequence of $Q_{st}$ of $N_2$ agrees well with the sequence of $N_2$ adsorption capacity, that is, pillar[6]arene_N4 ($\sim$ 13) > pillar[6]arene_N2 ($\sim$ 12) > pillar[6]arene ($\sim$ 11). For $CO_2$ and $N_2$, the $Q_{st}$ analysis clearly shows that the adsorption capacity of gases depends on the strength of the gas-framework interaction.

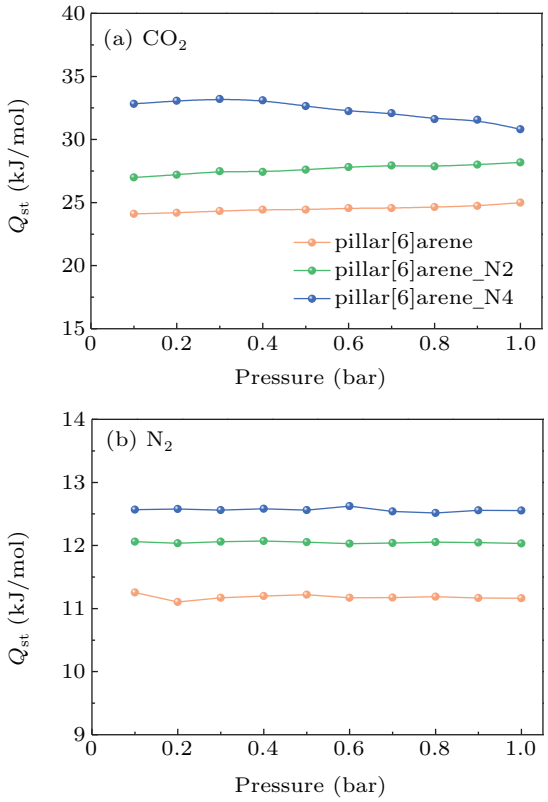



**Fig. 5.** Isosteric heat of $CO_2$ and $N_2$ on the azo-based pillar[6]arenes at 298 K.

To estimate intrinsic of the interaction between $CO_2/N_2$ and frameworks in detail, Coulomb and van der Waals interactions of gas–framework in azo-based pillar[6]arenes are calculated in Fig. 6. The van der Waals interactions of $CO_2/N_2$–framework are relatively larger than the corresponding Coulomb interactions. The pillar[6]arene_N4 shows the maximal van der Waals and Coulomb interactions, which is larger than pillar[6]arene_N2 and pillar[6]arene for $CO_2/N_2$. For the $CO_2$, the van der Waals interaction of $CO_2$–framework in the pillar[6]arene is maximum ($\sim$ 16.11 kJ·mol$^{-1}$), which accounts for 74.79% contributions of the total interactions. The results show that the van der Waals interaction plays a leading role for the $CO_2$ adsorption capacity. The van der Waals interaction of $CO_2$ increase to $\sim$ 17.70 kJ·mol$^{-1}$ for pillar[6]arene_N2 and for $\sim$ 18.55 kJ·mol$^{-1}$ pillar[6]arene_N4 due to the N=N groups. The van der Waals and Coulomb interactions of $N_2$ are less than these of $CO_2$. The Coulomb

interaction between $N_2$ and framework is very small ($\sim$ 0.89–0.38 kJ·mol$^{-1}$), which is attributed to the weak electric quadrupole moment of $N_2$. The results reveal the nature mechanism of the difference between $CO_2$ and $N_2$ adsorption capacities.

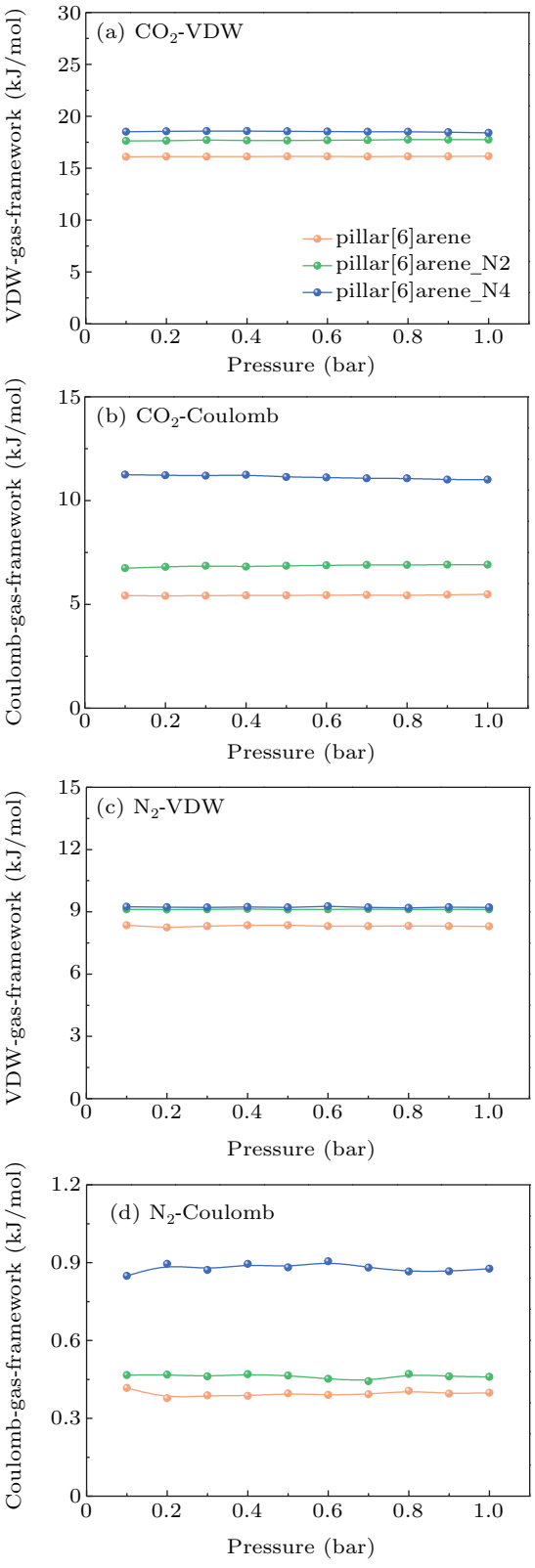



**Fig. 6.** Coulomb and van der Waals interactions of gas–framework in the azo-based pillar[6]arenes at 298 K. (a) and (c) Van der Waals interactions, (b) and (d) Coulomb interactions.

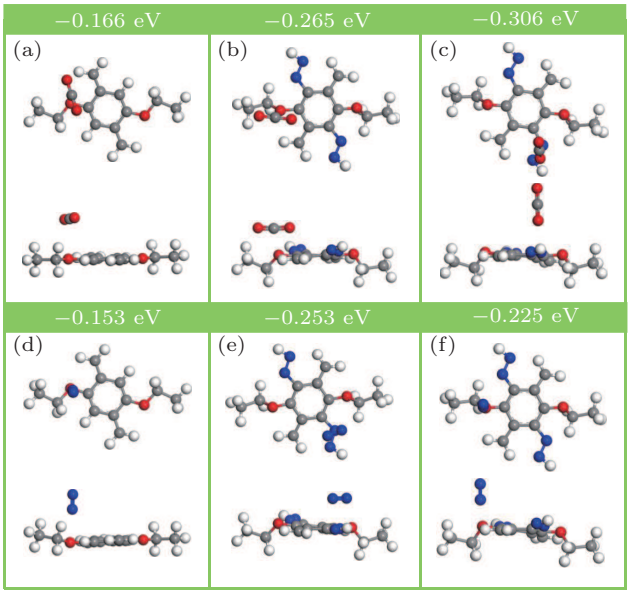



**Fig. 7.** Stable adsorption configurations $CO_2$ (a)–(c), and $N_2$ (d)–(f) at different sites.

To understand the interaction between $CO_2/N_2$ and each part in the azo-based pillar[6]arene surface, the adsorption energy ($E_{ads}$) is explored by DFT simulation. $E_{ads}$ is obtained by the following equation:[44]

$$E_{ads} = E_{gas+surf} - E_{gas} - E_{surf}, \tag{7}$$

where $E_{gas}$ is the energy of the gas molecule, $E_{surf}$ is the energy of fragment in the azo-based pillar[6]arenes, and $E_{gas+surf}$ is the total energy of the gas molecule adsorbed on the fragment of azo-based pillar[6]arens. Based on the definition, a larger negative value represents the more stable adsorption. The macrocyclic backbone are cut off from the initial and azo-based pillar[6]arenes to illustrate the effect of O and N atom on $CO_2/N_2$ molecules. The most stable adsorption configuration of $CO_2$ in the fragment of initial pillar[6]arene is shown in Fig. 7(a), $CO_2$ is adsorbed on the top of O atom, and the corresponding adsorption energy is −0.166 eV. For the azo-based pillar[6]arene, the most stable adsorption configuration of $CO_2$ in the fragment of azo-based pillar[6]arene is that $CO_2$ is adsorbed on the top of N atom in the N=N group, and the corresponding adsorption energy is −0.306 eV in Fig. 7(c). In addition, the $CO_2$ adsorbed on the top of O atom in the azo-based pillar[6]arene is calculated, and the adsorption energy is −0.265 eV in Fig. 7(b). Comparing with initial framework, azo-functionalization increase the interaction between $CO_2$ and O atom in the frameworks, and the N atoms in N=N group provide most stable adsorption configuration of $CO_2$. For $N_2$ molecule, the most stable adsorption configuration of $N_2$ in the fragment of initial pillar[6]arene is that $CO_2$ is adsorbed on the top of O atom, and the corresponding adsorption energy is −0.153 eV in Fig. 7(d). This value is smaller than that of the azo-based pillar[6]arene (−0.225 eV). $CO_2$ is adsorbed on the top of N atom in the N=N group, that is,

the most stable adsorption configuration of $N_2$ in the fragment of azo-based pillar[6]arene, and the corresponding adsorption energy is −0.253 eV in Fig. 7(e). In short, the introduction of N=N groups has a more positive influence on $CO_2/N_2$ for surface adsorption enhancement by inductive effect/direct interaction, especially for $CO_2$.

## 4. Conclusion

The effects of azo-functionalization on the adsorption and separation of $CO_2/N_2$ in pillar[6]arenes have been investigated by DFT and GCMC simulations. Azo-based pillar[6]arene provide a favorable environment for the separation of $CO_2/N_2$ by suitable pore sizes. The azo-based pillar[6]arene enhance the adsorption and separation capacity of $CO_2/N_2$. Adsorption capacity of $CO_2/N_2$ is more significantly enhanced by azo-functionalization, and the more N=N group leads to the more adsorption capacity. The isosteric heat and adsorption energy show that azo-functionalization can effectively increase the interaction between $CO_2/N_2$ and pillar[6]arene. The interaction analysis shows that azo-functionalization enhance the van der Waals and Coulomb interaction, and van der Waals interaction of gas is higher than the Coulomb interaction. This work highlights the effects of azo-functionalization on the adsorption and separation of $CO_2/N_2$ in pillar[6]arenes, and provides an effective strategy for designing and screening adsorbent materials for carbon capture and separation.

## References


[1] Oschatz M and Antonietti M 2018 *Energy Environ. Sci.* **11** 57
[2] Kupgan G, Abbott L J, Hart K E and Colina C M 2018 *Chem. Rev.* **118** 5488
[3] Lu X Q, Jin D L, Wei S X, Wang Z J, An C H and Guo W Y 2015 *J. Mater. Chem. A* **3** 12118
[4] Patil R S, Banerjee D, Zhang C, Thallapally P K and Atwood J L 2016 *Angew. Chem. Int. Ed.* **128** 4599
[5] Dewal M B, Lufaso M W, Hughes A D, Samuel S A, Pellechia P and Shimizu L S 2006 *Chem. Mater.* **18** 4855
[6] Lim S, Kim H, Selvapalam N, Kim K J, Cho S J, Seo G and Kim K 2008 *Angew. Chem. Int. Ed.* **120** 3400
[7] Li E, Jie K C, Zhou Y J, Zhao R and Huang F H 2018 *J. Am. Chem. Soc.* **140** 15070
[8] Ogoshi T, Saito K, Sueto R, Kojima R, Hamada Y, Akine S, Moeljadi A M P, Hirao H, Kakuta T and Yamagishi T 2018 *Angew. Chem. Int. Ed.* **57** 1592
[9] Ogoshi T, Sueto R, Yoshikoshi K and Yamagishi T 2014 *Chem. Commu.* **50** 15209
[10] Tan L L, Zhu Y L, Long H, Jin Y H, Zhang W and Yang Y W 2017 *Chem. Comm.* **53** 6409
[11] Tan L L, Zhu Y L, Jin Y H, Zhang W and Yang Y W 2018 *Supramol. Chem.* **30** 648
[12] Jursic B S 1998 *J Mol Struct: THEOCHEM* **452** 145
[13] Potoff J J and Siepmann J I 2001 *AIChE J.* **47** 1676
[14] Mayo S L, Olafson B D and Goddard W A 1990 *J. Phys. Chem.* **94** 8897
[15] Li X F, Zhu L, Xue Q Z, Chang X, Ling C C and Xing W 2017 *ACS Appl. Mater. Interfaces* **9** 31161
[16] Wu Z H, Wei S X, Wang M H, Zhou S N, Wang J H, Wang Z J, Guo W Y and Lu X Q 2018 *J. CO2 Util.* **28** 145
[17] Salavati M, Ghasemi H and Rabczuk T 2018 *Comput. Mater. Sci.* **149** 460
[18] Dubbeldam D, Calero S, Ellis D E and Snurr R Q 2016 *Mol. Simulat.* **42** 81
[19] Kumar K V, Preuss K, Lu L H, Guo Z X and Titiricit M M 2015 *J. Phys. Chem. C* **119** 22310
[20] Sarkisov L and Harrison A 2011 *Mol. Simulat.* **37** 1248
[21] Düren T, Millange F, Férey G, Walton K S and Snurr R Q 2007 *J. Phys. Chem. C* **111** 15350
[22] Garshasbi V, Jahangiri M and Anbia M 2017 *Appl. Surf. Sci.* **393** 225
[23] Zhang S Y, Jensen S, Tan K, Wojtas L, Roveto M, Cure J, Thonhauser T, Chabal Y J and Zaworotko M J 2018 *J. Am. Chem. Soc.* **140** 12545
[24] Wu X W, Han X, Liu YH, Liu Y and Cui Y 2018 *J. Am. Chem. Soc.* **140** 16124
[25] Gopalsamy K and Subramanian V 2018 *New J. Chem.* **42** 4240
[26] Thommes M, Kaneko K, Neimark A V, Olivier J P, Rodriguez-Reinoso F, Rouquerol J and Sing K S W 2015 *Pure Appl. Chem.* **87** 1051
[27] Chaix A, Mouchaham G, Shkurenko A, Hoang P, Moosa B, Bhatt P M, Adil K, Salama K N, Eddaoudi M and Khashab N M 2018 *J. Am. Chem. Soc.* **140** 14571
[28] Tan L L, Li H W, Tao Y C, Zhang X A, Wang B and Yang Y W 2014 *Adv. Mater.* **26** 7027
[29] Dai J J, Xie D Y, Liu Y, Zhang Z G, Yang Y W, Yang Q W, Ren Q L and Bao Z B 2020 *Ind. Eng. Chem. Res.* **59** 7866
[30] Zhou S N, Guo C, Wu Z H and Wang M H 2017 *Appl. Surf. Sci.* **410** 259
[31] Chen S J, Fu Y, Huang Y X and Tao Z C 2016 *J. Porous. Mat.* **23** 713
[32] Balbuena P B and Gubbins K E 1993 *Langmuir* **9** 1801
[33] Prasetya N, Donose B C and Ladewig B P 2018 *J. Mater. Chem. A* **6** 16390
[34] Patel H A, Je S H, Park J, Chen D P, Jung Y S, Yavuz C T and Coskun A 2013 *Nat. Commun.* **4** 1357
[35] Hu J B, Liu Y, Liu J, Gu C K and Wu D W 2018 *Fuel* **226** 591
[36] Chokbunpiam T, Fritzsche S, Chmelik C, Caro J, Janke W and Hannongbua S 2016 *J. Phys. Chem. C* **120** 23458
[37] Li J R, Kuppler R J and Zhou H C 2009 *Chem. Soc. Rev.* **38** 1477
[38] Yang X, Rees R J, Conway W, Puxty G and Winkler D A 2017 *Chem. Rev.* **117** 9524
[39] Arab P, Rabbani M, Sekizkardes A K and Islamoglu T 2014 *Chem. Mater.* **26** 1385
[40] Patel H A, Je S H, Park J, Jung Y S, Coskun A and Yzvuz C T 2013 *Chem. A Eur. J.* **20** 772
[41] Liu B, Yao S, Liu X Y, Li X, Krishna R, Li GH, Huo Q S and Liu Y L 2017 *ACS Appl. Mater. Interfaces* **9** 32820
[42] Rahimi M, Singh J K and Müller-Plathe F 2016 *Phys. Chem. Chem. Phys.* **18** 4112
[43] Watabe T and Yogo K 2013 *Sep. Purif. Technol.* **120** 20
[44] Zhu F, Dong S and Cheng G 2011 *Chin. Phys. B* **20** 077103